Trans Indian Inst Met (2022) 75(8):2129–2137
https://doi.org/10.1007/s12666-022-02578-6

ORIGINAL ARTICLE

Contribution of Mechanical Activation on the Growth of Intermetallic Compound Layers at the Cu/Al Interface During Vacuum Hot Pressing

Shao-peng Wu[1] · Xiao-lan Cai[1] · Lei Zhou[1] · Chang-jiang Yang[1] · Wen-hao Li[1] · Yuan-chao Cheng[1]

Received: 26 October 2021 / Accepted: 3 March 2022 / Published online: 6 April 2022
© The Indian Institute of Metals - IIM 2022

Abstract In the present paper, the Cu/Al diffusion couples were successfully prepared using high-energy ball milling and vacuum hot pressing sintering. The aim of this study was to investigate the influence of mechanical activation on the growth of intermetallic compound layers at the Cu/Al interface during hot pressing. Various results were obtained via X-ray diffractometry and field emission scanning electron microscopy analysis. Results showed that from the Cu side to Al side, Cu_9Al_4, CuAl, and $CuAl_2$ phases can be identified successively at the interface. In particular, a large number of pores are dispersed in the Cu matrix and Cu_9Al_4 layer of the samples after ball milling, and the interface between Cu and Cu_9Al_4 phase is blurred. In addition, compared with the unmilled sample, the thickness of the intermetallic compound layer at the Cu/Al interface of the ball-milled sample increases significantly. In terms of a single layer, although mechanical activation can improve atomic diffusivity, the growth of intermetallic compound layer is also affected by holding time. Due to the different relative positions of various intermetallic compounds at the interface, the thickness of the intermetallic compound layer near the Cu side increases significantly with a shorter holding time, while the thickness of the intermetallic compound layer near the Al side requires a longer holding time.

Keywords Cu/Al interface · Intermetallic compounds · Powder metallurgy · Mechanical activation · Hot pressing

✉ Xiao-lan Cai
kmustcxl@163.com

[1] Faculty of Metallurgical and Energy Engineering, Kunming University of Science and Technology, Kunming 650093, Yunnan, China

1 Introduction

Copper/aluminum clad composites combine the advantages of high thermal and electrical conductivity of copper and low density and corrosion resistivity of aluminum. They have been widely used for bus bar conductors, heat sink, armored cable, and so on [1–3]. Cu/Al clad is recognized as one of the most promising alternatives to pure copper for automotive applications[4]. Various processes have been commonly utilized for the preparation of copper–aluminum clad composites, such as explosive bonding [5, 6], diffusion bonding [7], friction stir welding [8–10], severe plastic deformation [11], chemical vapor deposition [12], continuous casting [13, 14], roll bonding [15–17], and hot pressing [18].

After being in contact, copper and aluminum will diffuse each other due to the different chemical natures, and one or several intermediate compounds (IMCs) are usually formed at the Cu/Al interface with a layered form. In addition, the interdiffusion between different materials may lead not only to the formation of compounds but also to the generation of vacancies, which is called the Kirkendall effect [7]. Previous research has established that various investigation techniques may form Cu_9Al_4, CuAl, $CuAl_2$, and other IMCs at the Cu/Al interface. Among them, the order of formation of Cu_9Al_4 and $CuAl_2$ phases is very different from that of Cu–Al powder by mechanical alloying method [19], which may be related to the interface scale of diffusion couples. Guo et al. [20] studied the formation of IMCs at the Cu/Al interface after holding for 10–30 min in the temperature range of 673–773 K by plasma-activated sintering. The results show that the $CuAl_2$ phase is first precipitated on the Cu/Al interface, which is consistent with that in the Al–Cu system studied by Xu et al.[21]. θ-$CuAl_2$ is the first IMC to nucleate, and then the

Cu_9Al_4 phase is precipitated at the α-Cu(Al)/$CuAl_2$ interface. Lee et al. [18] realized the diffusion bonding of Cu and Al at the temperature of 623–923 K by vacuum hot pressing process. When the temperature is lower than 823 K, the bonding between the Cu and Al layers is insufficient. After the temperature rises to 873 K, there is no obvious delamination at the Cu/Al interface. With the further increase in the process temperature, the thickness of the diffusion-induced Cu/Al interface layer increases significantly. Similar results can be found in Chen's study [22] of characterizing $CuAl_2$ near the Al side, Cu_9Al_4 near the Cu side, and CuAl+Cu_4Al_3 as the intermediate layer. However, these methods all use Cu and Al sheets as raw materials, first grinding and polishing for the diffusion surface to remove the oxide film [23] and then conducting experiments. However, after the above treatment, it is difficult to ensure the flatness of the Cu/Al interface at the micro-level, which may be the main reason for the weak bonding of Cu/Al diffusion couple and the formation of cracks of Cu/Al interface [7]. In addition, the IMCs of the multilayer structure formed at the Cu/Al interface present an irregular interface, and the thickness of each IMC layer is not uniform [17, 20].

Previous studies have shown that the movement of the Cu atom is a factor that limits the formation of IMCs during the migration of Cu/Al interface atoms [20]. Therefore, the ball milling process is used to pretreat the Cu powder to improve the atomic diffusivity. An objective of this study is to investigate the effect of mechanical activation on the growth of IMC layers at the Cu/Al interface during hot pressing. The two-step hot pressing sintering process is used to solve the problems that the Cu/Al interface is not well bonded.

2 Materials and Methods

2.1 Preparation of Pure Cu Slabs

Add 100 g of commercial-purity Cu powders (99.8% purity, 75 μm, Changsha Tianjiu Metal Materials Co., Ltd.) to a horizontal high-energy stirring ball mill (HCX-1L, Kunming HCX Science and Technology Co., Ltd.), and at the same time add 1 kg, 3 mm zirconium balls as grinding medium, in which the ball-to-powder ratio was maintained at 10:1. The whole ball milling process was carried out under the protection of Ar gas using an unconventional alternating speed of 2000/2100 rpm. The equipment contained a cooling system, which can control the temperature at 298 ± 3 K. To prevent the powder from sticking to both the balls and vial walls, stearic acid was added to the container at 1 wt% of the total mass of the Cu powders as a process control agent. In addition, to increase the Cu atom diffusivity, they were ball-milled for 30 and 60 min, respectively, and compared with the unmilled samples. 10 g of the ball-milled Cu powder was put into a graphite mold with an inner diameter of 30 mm, and then the mold was put in a vacuum hot-press sintering furnace for sintering. The powders were consolidated at 1073 K for 60 min with an applied pressure of 50 MPa, and the vacuum degree was not higher than 8.5×10^{-3} Pa.

2.2 Preparation of Cu/Al Diffusion Couples

Sandpaper was used to polish the surface of the sintered Cu slabs in the order of 400, 800, 1000, 1500, 2000, 3000, and then polished with 1 μm and 0.5 μm diamond paste, and finally cleaned with acetone in an ultrasonic bath. The purpose of grinding and polishing was not only to make the surface of the Cu slabs smooth but also to remove the surface oxide layer and other surface impurities. Immediately after the washing, the Cu slabs were dried. The processed Cu slab was put into a graphite mold, and then 3.5 g of pure-Al powders (99.8% purity, 8–12 μm, Changsha Tianjiu Metal Materials Co., Ltd.) was put on the Cu slab. The mold was placed in a hot-press sintering furnace for secondary sintering to prepare Cu/Al diffusion couples. The structure of the Cu slab and powders was consolidated at 773 K under the applied pressure of 30 MPa, and the vacuum degree remained the same as above. To study the formation and growth of IMCs in the Cu/Al diffusion couples, the samples were held for 10, 20, and 30 min, respectively. The parameters for the syntheses of all the samples used in this work are summarized in Table 1, for example, in Cu-MA-60/Al-30 specimen, MA refers to mechanical activation, 60 means mechanical activation time of 60 min, and 30 means hot pressing sintering holding time of 30 min. The preparation process of Cu/Al diffusion couples in this work is shown in Fig. 1.

2.3 Characterization

The phase compositions of the samples were detected with an X-ray diffractometer (XRD, Empyrean, Panalytical) using Cu Kα radiation. The morphology of the Cu/Al diffusion couples was observed using field emission scanning electron microscopy (FESEM, Nova Nano SEM 450, USA). The elemental composition was investigated using an energy-dispersive X-ray spectrometer (EDX).

Table 1 The parameters for the syntheses of all the samples

Number	1. Milling time (min)	2. Sintering time (min)	Materials
1	0	10	Cu/Al-10
2	30	10	Cu-MA-30/Al-10
3	60	10	Cu-MA-60/Al-10
4	0	20	Cu/Al-20
5	30	20	Cu-MA-30/Al-20
6	60	20	Cu-MA-60/Al-20
7	0	30	Cu/Al-30
8	30	30	Cu-MA-30/Al-30
9	60	30	Cu-MA-60/Al-30

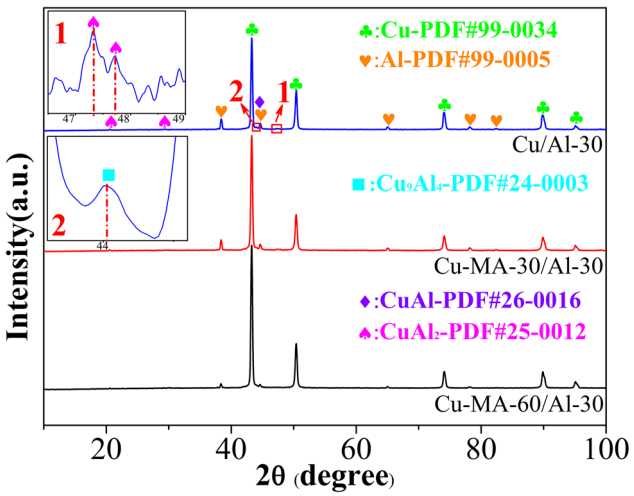

Fig. 2 XRD patterns of Cu/Al diffusion couples prepared by ball milling of pure Cu for different times

3 Results and Discussion

3.1 Identification of Phases

Figure 2 shows the XRD patterns under the micro-region X-ray diffraction (micro-XRD) from the Cu/Al diffusion couple Cu/Al-30, Cu-MA-30/Al-30, and Cu-MA-60/Al-30 specimens. The specimens exhibit similar peaks corresponding to Cu, Al, Cu_9Al_4, CuAl, and $CuAl_2$ phases, respectively. Peaks for other IMCs (Cu_4Al_3 phase) are not observed in the XRD patterns, which is consistent with the results of Kim et al. [17]. Further studies are needed to prove the formation of IMCs at the Cu/Al interface under experimental conditions.

3.2 Interfacial Microstructure

To further investigate the formation and growth of IMCs, backscattered electron micrographs of samples were used to directly observe their formation and growth at the Cu/Al interfaces, as shown in Fig. 3. The brighter and darker zones indicate pure-Cu and pure-Al regions, respectively, while the grey zone reflects the IMC layer formed under the experimental conditions. From the FESEM images and the corresponding EDX analysis in Fig. 3a, d, g, three kinds of IMCs are formed at the Cu/Al interface. According to the atomic ratio of Cu and Al in different positions in all specimens (see Table 2), three kinds of layered IMCs can be identified as Cu_9Al_4 phase close to the Cu side, $CuAl_2$ phase close to the Al side, and CuAl phase formed at the $Cu_9Al_4/CuAl_2$ interface, which is consistent with the above micro-XRD analysis. In addition, it can be seen from Fig. 3 that the Cu/Al interface is well bonded without delamination, which also proves that the two-step vacuum hot pressing sintering process can effectively solve the interface delamination problem reported in the literature. Specifically, the boundary between the four layers of

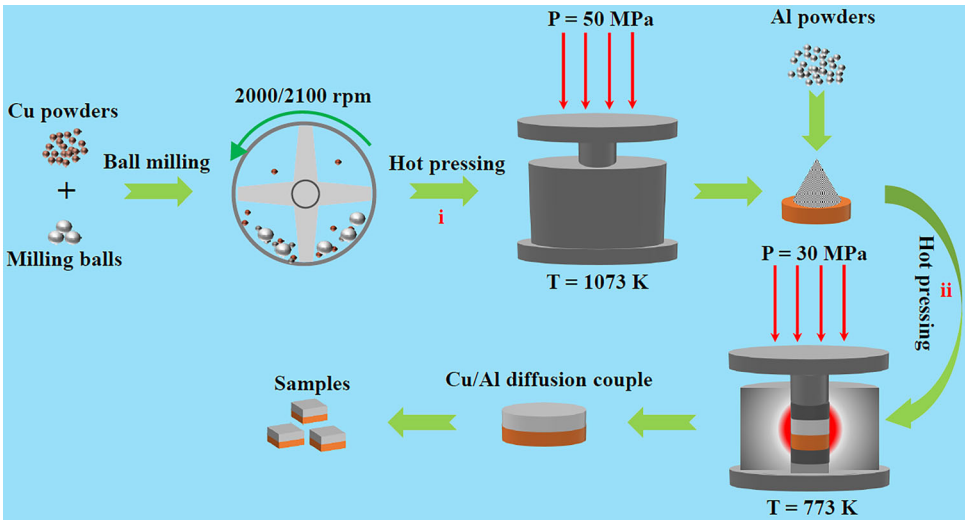

Fig. 1 Preparation process of Cu/Al diffusion couples

Cu_9Al_4, CuAl, $CuAl_2$, and Al can be seen in the diffusion couples after ball milling, but the boundary between Cu matrix and Cu_9Al_4 phase is difficult to identify on the micro-scale. Moreover, compared with unmilled samples, a large number of pores are observed in the ball-milled samples, and the number of pores increases with the increase in the ball-milling time. The following will conduct a more in-depth study and discussion of the above results.

In this study, the IMCs are formed during the secondary hot pressing sintering process. The purpose of pre-ball milling Cu powder by mechanical activation is to increase the atomic diffusivity, thereby promoting the growth of the IMC layers. It is also interesting to see that in Fig. 4, many pores can be observed in the Cu and Cu_9Al_4 regions. It is well known that during the sintering process, due to inappropriate process parameters, the relative density of the sintered sample will decrease, which manifests as a large number of voids in the microstructure of the sample. In this paper, compared with Cu-MA-60/Al-20 sample, the sintering parameters are consistent, and no pores are observed in the Cu/Al-20 sample (Fig. 3d). Compared with the Cu-MA-60/Al-20 sample, the sintering temperature and pressure are consistent during the sintering process. After reducing the sintering time by 10 min, the pores are also not observed in the Cu/Al-10 sample (Fig. 3a), which greatly reduces the influence of the sintering process on the formation of the pores. Compared with Fig. 3a, d, g, the samples without ball milling do not have pores formation with the extension of holding time in the sintering process. Compared with Fig. 3a–c, under the same sintering process conditions, with the increase in mechanical activation time, the number of the pores gradually increases. Compared with Fig. 3c, f, i, under the same ball milling conditions, with the increase in holding time during sintering, the number of pores also increases. The above comparison results show that mechanical activation is the primary condition for the generation of pores, and during the subsequent sintering process, the number of pores increases and the corresponding size also increases. The ball milling process can destroy the crystal structure of the material, thereby generating a large number of vacancies and other defects [24, 25]. During the first step of sintering to prepare Cu sheets, some defects are recovered, but many defects are preserved. During the subsequent secondary sintering to prepare the Cu/Al diffusion couples, due to the coalescence of vacancies formed by the different atomic fluxes across the Cu/Al interface [7], the pores can be observed on the micro-level. Specially, the Cu_9Al_4 is a rather complex phase, which nucleates inside the Cu-rich supersaturated solid solution matrix rather than at the Cu/Al interfaces. These pores are uniformly presented in the Cu_9Al_4 layer

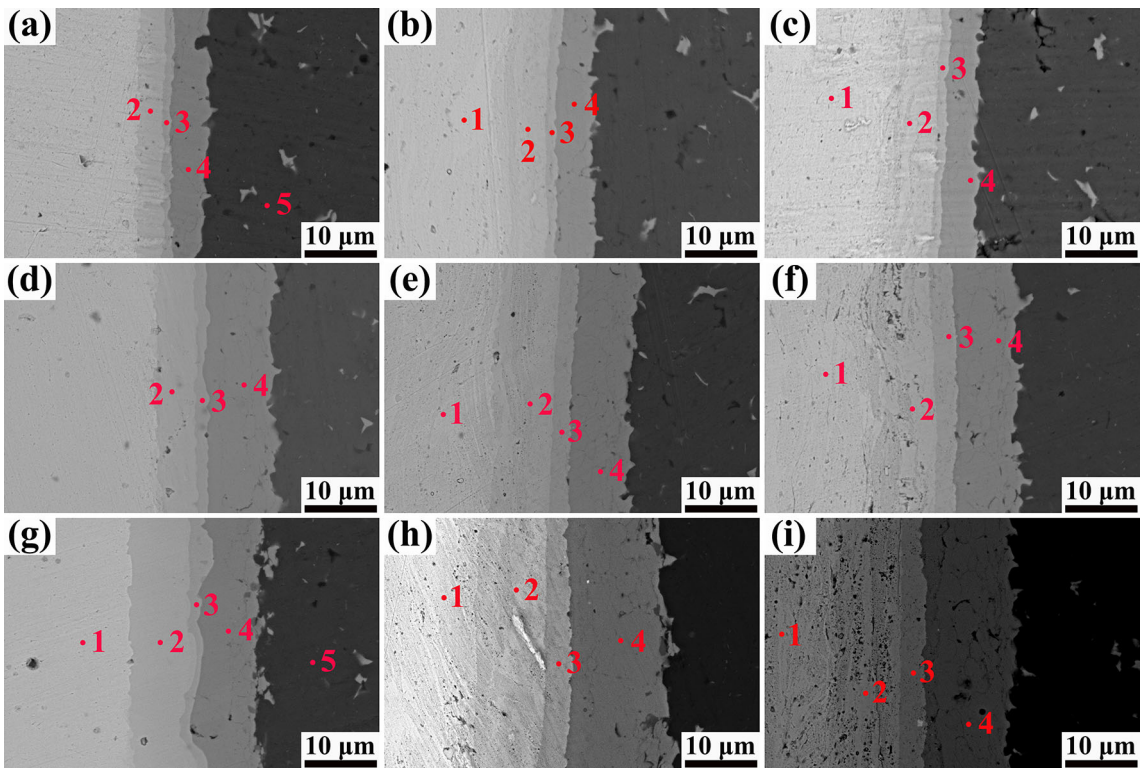

Fig. 3 FE-SEM micrographs observed from the interface of specimens. **a** Cu/Al-10, **b** Cu-MA-30/Al-10, **c** Cu-MA-60/Al-10, **d** Cu/Al-20, **e** Cu-MA-30/Al-20, **f** Cu-MA-60/Al-20, **g** Cu/Al-30, **h** Cu-MA-30/Al-30, **i** Cu-MA-60/Al-30

Table 2 EDX analysis of the local zones indicated in Fig. 3

Regions		Sample number								
		1	2	3	4	5	6	7	8	9
1	Cu (at.%)	–	100.0	97.3	–	100.0	100.0	100.0	97.1	97.7
	Al (at.%)	–	–	2.7	–	–	–	–	2.9	2.3
2	Cu (at.%)	64.3	63.6	69.8	64.8	63.1	64.6	64.7	64.3	66.5
	Al (at.%)	35.7	36.4	30.2	35.2	36.9	35.4	35.3	35.7	33.5
3	Cu (at.%)	51.5	51.7	53.0	51.4	50.7	51.8	53.8	52.0	51.3
	Al (at.%)	48.5	48.3	47.0	48.6	49.3	48.2	46.2	48.0	48.7
4	Cu (at.%)	34.6	34.3	31.3	34.5	34.1	34.5	34.8	34.4	34.6
	Al (at.%)	65.4	65.7	68.7	65.5	65.9	65.5	65.2	65.6	65.4
5	Cu (at.%)	–	–	–	–	–	–	–	–	–
	Al (at.%)	100.0	–	–	–	–	–	100.0	–	–

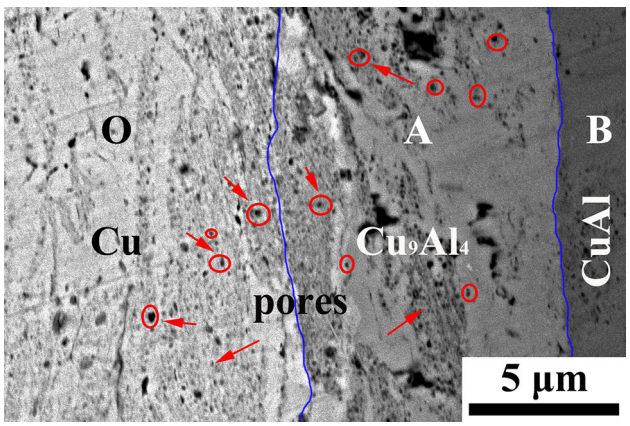

Fig. 4 FE-SEM micrograph observed from the interface of Cu-MA-60/Al-20 specimen magnified 20,000 times

with the formation and growth of the Cu_9Al_4 layer, which also causes the Cu/Cu_9Al_4 interface to be unclear.

Figure 5 shows the SEM micrographs and EPMA line/mapping analysis of the Cu/Al interface microstructures. As can be seen from Fig. 5a, d, g, five obvious platforms can be found on the EPMA line spectra of Cu and Al, corresponding to the five-layer structure of the Cu/Al interface of the sample without ball milling, respectively, which is consistent with the above research results. It is interesting to see that in Fig. 5b, c, the Cu/Cu_9Al_4 interface of the samples after ball milling is difficult to observe only in the FESEM image, and the Cu/Cu_9Al_4 interface becomes more blurred as the ball-milling time increases. Figure 5e, h corresponds to the EPMA mapping of Al and Cu of Cu-MA-30/Al-30, respectively. In Fig. 5e, the interface between the Cu matrix and the Cu_9Al_4 phase is clearly observed. Similarly, the Cu/Cu_9Al_4 interface in the Cu-MA-60/Al-30 sample can be observed through the EPMA mapping (as shown in Fig. 5f, i). This provides favorable conditions for the subsequent determination of the thickness of the IMC layers.

3.3 Formation of IMCs and Promoting Mechanism of Mechanical Activation on IMC Layers Growth

In the case of the Cu–Al system, due to interdiffusion, saturated solid solutions of Cu(Al) and Al(Cu) formed on each side. In particular, the solubility limit of Al in Cu is 19.7 at.% in the temperature for 773 K, while the maximum solubility limit of Cu in Al in the same temperature is only 2.48 at.% [26]. Since the solubility limit of Cu in Al is much lower than that of Al in Cu, the Al(Cu) solid solution would be expected to saturate first, resulting in the nucleation of $CuAl_2$, as experimentally observed by a previous study [22]. Then, the Cu_9Al_4 phase is preferentially formed at the interface of Cu(Al)/$CuAl_2$ because the driving force for the formation of Cu_9Al_4 is greater than those for the

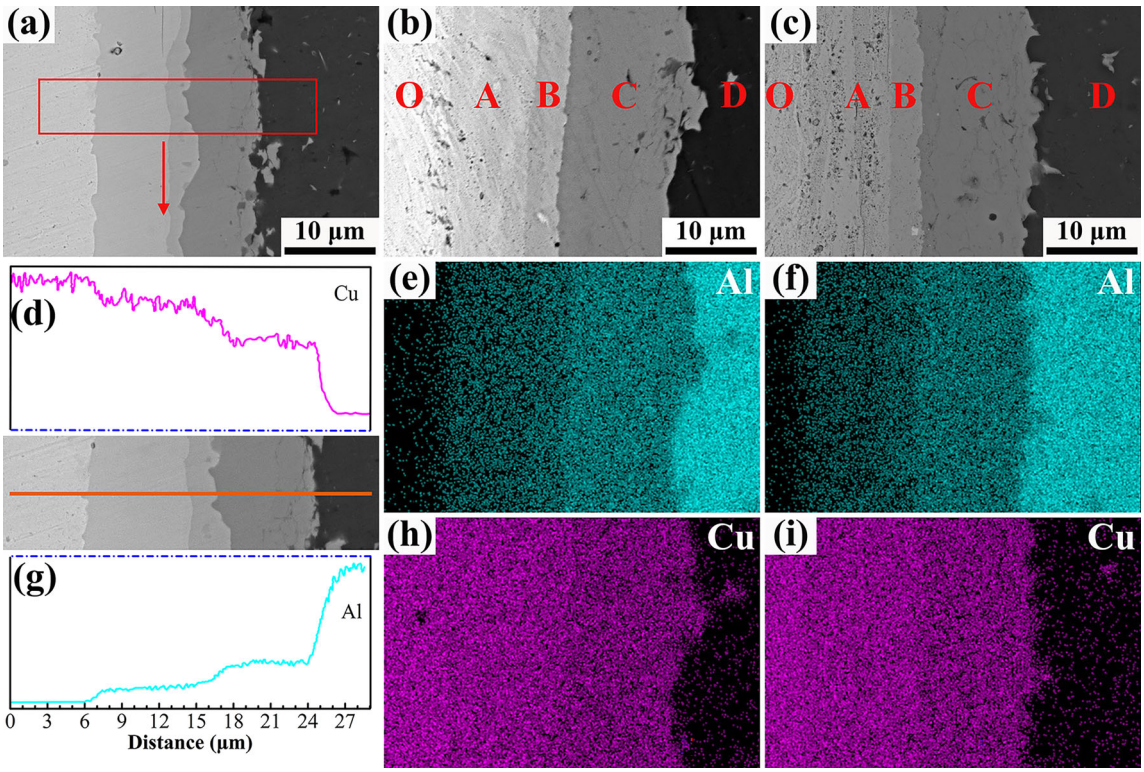

Fig. 5 **a, d, g** EPMA line analysis of Cu/Al-30 specimen, **b, e, h** EPMA mapping analysis of Cu-MA-30/Al-30 specimen, **c, f, i** EPMA mapping analysis of Cu-MA-60/Al-30 specimen

other phases at 773 K. Finally, the CuAl phase is formed on the $Cu_9Al_4/CuAl_2$ interface in the same way [20]. In terms of the microstructure of the Cu/Al interface, Cu_9Al_4 phase is formed on the side close to Cu, $CuAl_2$ phase is formed on the side close to Al, and CuAl phase is formed between Cu_9Al_4 and $CuAl_2$ phases, which is consistent with the results in this study and indirectly proves the formation mechanism of IMCs in the study process. The distribution of the IMC layers is shown in Fig. 6.

Moreover, the nucleation and growth of the new phase require atoms to rearrange into the particular crystal structure of that phase [27]; so different levels of atomic mobility may be required, and atomic mobility is positively correlated with temperature. The whole diffusion process must be carried out in a high-temperature environment for high atomic mobility. In previous studies, it was found that IMC layers could be observed at Cu/Al interface only when the temperature exceeded 873 K [18]. However, the mechanical activation process can effectively reduce the reaction potential energy and thus activate the solid-state reaction [28, 29]. Moreover, the major function of mechanical milling is to enhance the atomic diffusivity by creating a large number of structural defects that include vacancies, dislocations, and grain boundaries [27, 30]. In this study, the effect of mechanical activation on the growth of the IMC layer was studied. Compared with Fig. 6a, b, the thickness of IMC layers increases significantly after 30 min of ball milling. As shown in the schematic diagram of Fig. 6, the appearance of pores in the sample after ball milling confirms the existence of structural defects, which makes the increase in atomic diffusivity, and further leads to an increase in the thickness of the compound layers. However, the growth of IMC layers during sintering is controlled by the diffusion of Cu and Al atoms through the IMC layer [23] so that the thickness of the finally formed IMC layer is different.

3.4 Thickness of IMC Layers

In the process of vacuum hot pressing, the formation and growth of IMC layers on the Cu/Al interface can be expressed by the following chemical half-reaction equations:

$$Al + Cu \rightarrow Al(Cu) \quad (1)$$

$$Cu + Al \rightarrow Cu(Al) \quad (2)$$

$$Cu + Al(Cu) \rightarrow CuAl_2 \quad (3)$$

$$Cu(Al) + CuAl_2 + Al \rightarrow Cu_9Al_4 \quad (4)$$

$$Cu_9Al_4 + CuAl_2 + Cu + Al \rightarrow CuAl \quad (5)$$

The IMC layers grow with the progress of the above reaction. Figure 7 shows the variation of IMC thicknesses

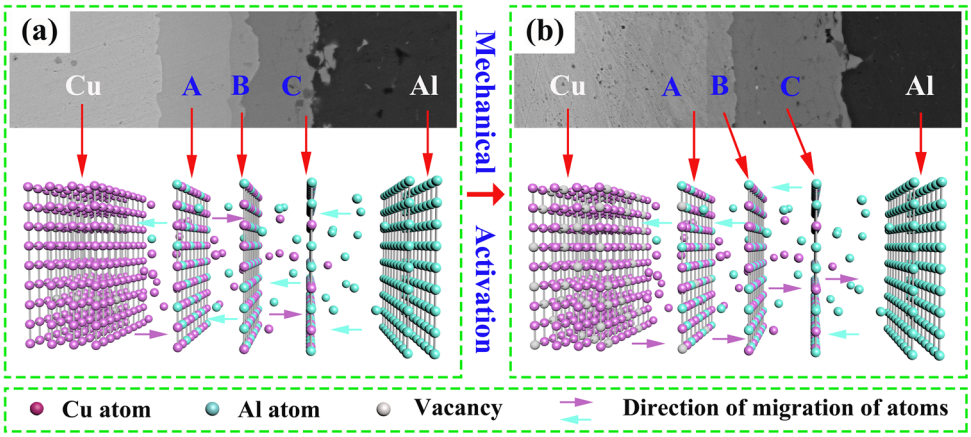

Fig. 6 Schematic of IMC layers formation and growth at Cu/Al interface: **a** Cu/Al-30, **b** Cu-MA-30/Al-30

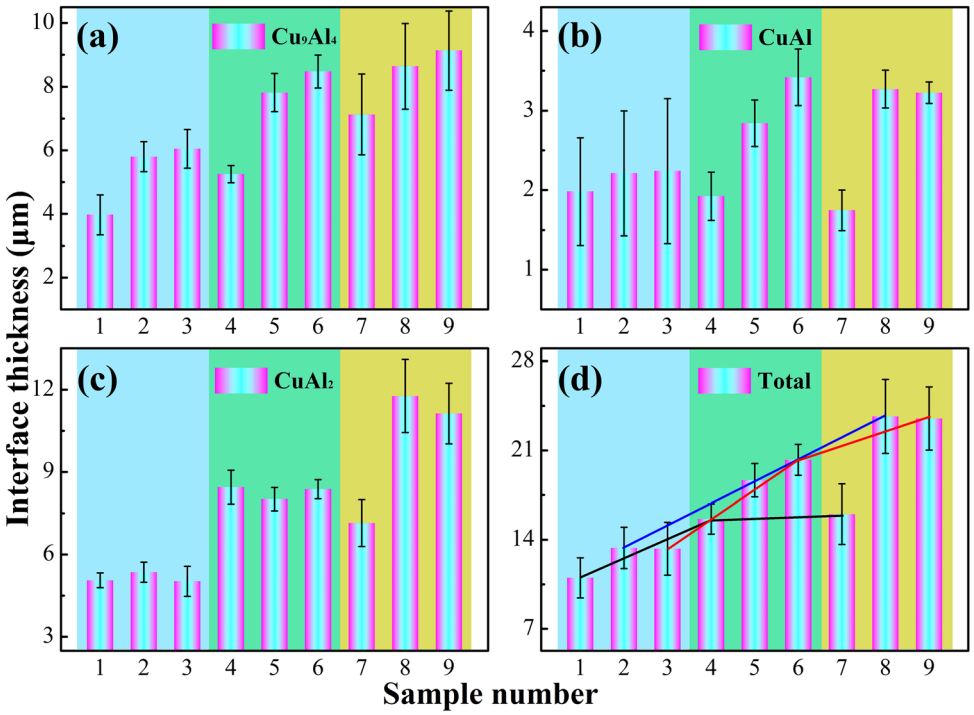

Fig. 7 Growth thickness of IMC layers as annealed at 773 K with different samples. **a** Cu_9Al_4 layer, **b** CuAl layer, **c** $CuAl_2$ layer, and **d** Total

as a function of milling time and annealing time at 773 K determined at Cu/Al interfaces. As can be seen from Fig. 7d, the growth of IMC layers follows the parabolic rule (black line) with the sintering time from 10 to 30 min in the samples without ball milling. However, after ball milling for 30 min and 60 min, respectively, the thickness of IMC layers increases significantly with the increase in holding time, and mechanical activation treatment make the parabola move forward. Namely, under the experimental conditions in this paper, the change of IMC thickness with time conforms to the law of the rapid growth stage of the first part of the parabola (red line and blue line), which also proves that the mechanical activation has a promoting effect on the growth of IMC layers. From the perspective of microstructure, the IMC layers at the Cu/Al interface are Cu_9Al_4 near the Cu side, $CuAl_2$ near the Al side, and CuAl in the middle. Although the MA process can improve the mobility of Cu atoms, the rate of atomic diffusion through the IMC layer during sintering is controlled by the temperature as well as the holding time. However, in this study, the temperature is set at 773 K, so the growth of the IMC layer is mainly affected by the holding time. Comparative analysis in Fig. 7a–c (combined with Table 3) shows that when the sintering time is less than 10 min, the thickness of Cu_9Al_4 layer adjacent to the Cu matrix increases obviously, but the rate of atomic diffusion through CuAl layer and $CuAl_2$ layer is limited, resulting in a small increase in the thickness of the two

Table 3 The thickness of IMC layers under experimental conditions (unit: μm)

Thickness	Ball milling time/min											
Sintering time /min	0				30				60			
	Cu_9Al_4	CuAl	$CuAl_2$	Total	Cu_9Al_4	CuAl	$CuAl_2$	Total	Cu_9Al_4	CuAl	$CuAl_2$	Total
10	3.97	1.98	5.06	11.01	5.80	2.21	5.35	13.36	6.04	2.23	5.02	13.29
20	5.25	1.92	8.45	15.62	7.81	2.84	8.01	18.66	8.47	3.42	8.37	20.26
30	7.12	1.75	7.14	16.01	8.64	3.27	11.76	23.67	9.14	3.23	11.13	23.50

layers. When the sintering time is less than 20 min, the thickness of Cu_9Al_4 and CuAl layer increases obviously, while the thickness of $CuAl_2$ layer increases slightly. When the sintering time reaches 30 min, the thickness of all IMC layers increases obviously.

4 Conclusions

The present study was designed to determine the effects of mechanical activation on the growth of IMCs in the Cu/Al diffusion couples during vacuum hot pressing sintering. The formation of three IMCs can be observed at the Cu/Al interface, namely the Cu_9Al_4 phase near the Cu side, $CuAl_2$ phase near the Al side, and CuAl phase formed between Cu_9Al_4 and $CuAl_2$. In addition, mechanical activation and a two-step sintering process solve the problem of Cu/Al interfacial delamination. Moreover, for the ball-milled samples, although mechanical activation can improve atomic diffusivity by creating structural defects, the growth of intermetallic compound layer is also affected by holding time. Because of the different relative positions of various intermetallic compounds at the interface, there are differences in the growth of each intermetallic compound layer under different holding times. Moreover, the generation of vacancies leads to the proliferation of pores, which results in a large number of pores distributed in the Cu matrix and Cu_9Al_4 layer, resulting in the blurring of the Cu/Cu_9Al_4 interface.

Acknowledgements This work was financially supported by the Program for Innovative Research Team (in Science and Technology) in the University of Yunnan Province (No. 14051693), the Basic Research Project of Yunnan Province (Nos. 202021AS070049 and 202102AB080004), and the National Natural Science Foundation of China (No. 51864042).

References

1. Abbasi M, Taheri A K, and Salehi M T, *J Alloys Compd* **319** (2001) 233.
2. Sheng L Y, Yang F, Xi T F, Lai C, and Ye H Q, *Composites Part B* **42** (2011) 1468.
3. Sasaki T T, Morris R A, Thompson G B, Syarif Y, and Fox D, *Scr Mater* **63** (2010) 488.
4. Kim I K, and Hong S I, *Mater Des* **47** (2013) 590.
5. Paul H, Litynska-Dobrzynska L, Miszczyk M, and Prażmowski M, *Arch Metall Mater* **57** (2012) 1151.
6. Paul H, Faryna M, Prażmowski M, Bański R, Warstwie Z, Płyt P, and Wybuchowo Z, *Arch Metall Mater* **56** (2011) 463.
7. Hannech E B, Lamoudi N, Benslim N, and Makhloufi B, *Surf Rev Lett* **10** (2003) 677.
8. Li X W, Zhang D T, Qiu C, and Zhang W, *T Nonferr Metal Soc* **22** (2012) 1298.
9. Barekatain H, Kazeminezhad M, and Kokabi A H, *J Mater Sci Technol* **30** (2014) 826.
10. Tan C W, Jiang Z G, Li L Q, Chen Y B, and Chen X Y, *Mater Des* **51** (2013) 466.
11. Llorca-Isern N, Escobar A M, Roca A, and Cabrera J M, *Mater Sci Forum* **706-709** (2012) 1811.
12. Moon H K, Yoon J, Kim H, and Lee N E, *Met Mater Int* **19** (2013) 611.
13. Su Y J, Liu X H, Huang H Y, Wu C J, Liu X F, and Xie J X, *Metall Mater Trans B* **42** (2011) 104.
14. Su Y J, Liu X H, Wu Y F, Huang H Y, and Xie J X, *Int J Miner Metall Mater* **20** (2013) 684.
15. Peng X K, Heness G, and Yeung W Y, *J Mater Sci* **34** (1999) 277.
16. Heness G, Wuhrer R, and Yeung W Y, *Mater Sci Eng A* **483** (2008) 740.
17. Kim M J, Lee K S, Han S H, and Hong H I, *Mater Charact* **174** (2021) 111021.
18. Lee K S, and Kwon Y N, *T Nonferr Metal Soc* **23** (2013) 341.
19. Wu S P, Cai X L, Cheng Y C, and Zhou L, *J Electron Mater* **50** (2021) 4549.
20. Guo Y J, Liu G W, Jin H Y, Shi Z Q, and Qiao G J, *J Mater Sci* **46** (2011) 2467.
21. Xu H, Liu C, Silberschmidt V V, Pramana S S, White T J, and Chen Z, *Scr Mater* **61** (2009) 165.
22. Chen C Y, and Hwang W S, *Mater Trans* **48** (2007) 1938.
23. Lee W B, Bang K S, and Jung S B, *J Alloys Compd* **390** (2005) 212.

24. Lin S S, and Liao C N, *J Appl Phys* **110** (2011) 093707.
25. Fan G, Geng L, Feng Y, Cui X, and Yan X, *Microsc Microanal* **21** (2015) 953.
26. Murray J L, *Int Met Rev* **30** (1985) 211.
27. Zhang D L, and Ying D Y, *Mater Sci Eng A* **301** (2001) 90.
28. Suryanarayana C, *Prog Mater Sci* **46** (2001) 1.
29. Ying D Y, and Zhang D L, *J Alloys Compd* **311** (2000) 275.
30. Zhang B Q, Lu L, and Lai M O, *Phys B* **325** (2003) 120.

Publisher's Note Springer Nature remains neutral with regard to jurisdictional claims in published maps and institutional affiliations.